Journal Pre-proof

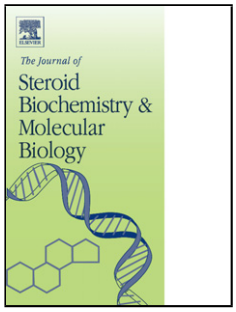

Role of human 3α-hydroxysteroid dehydrogenase isoforms (AKR1C1-AKR1C3) in the extrahepatic metabolism of the steroidal aromatase inactivator Formestane

Runlan Wan, Xi Kong, Youzhe Yang, Siwen Tao, Youyou Chen, Alexander Tobias Teichmann, Frank Heinrich Wieland

PII: S0960-0760(19)30246-8

DOI: https://doi.org/10.1016/j.jsbmb.2019.105527

Reference: SBMB 105527

To appear in: *Journal of Steroid Biochemistry and Molecular Biology*

Received Date: 30 April 2019

Revised Date: 31 October 2019

Accepted Date: 3 November 2019

Please cite this article as: Wan R, Kong X, Yang Y, Tao S, Chen Y, Teichmann AT, Wieland FH, Role of human 3α-hydroxysteroid dehydrogenase isoforms (AKR1C1-AKR1C3) in the extrahepatic metabolism of the steroidal aromatase inactivator Formestane, *Journal of Steroid Biochemistry and Molecular Biology* (2019), doi: https://doi.org/10.1016/j.jsbmb.2019.105527

Role of human 3α-hydroxysteroid dehydrogenase isoforms (AKR1C1-AKR1C3) in the extrahepatic metabolism of the steroidal aromatase inactivator Formestane

Runlan Wan[abc], Xi Kong[a], YouzheYang[a], Siwen Tao[d], Youyou Chen[e], Alexander Tobias Teichmann [a*], Frank Heinrich Wieland[a*] FHwieland@gmx.de

[a] Sichuan Provincial Center for Gynaecology and Breast Diseases, The Affiliated Hospital of Southwest Medical University, Luzhou 646000, China

[b] Nuclear Medicine and Molecular Imaging Key Laboratory of Sichuan Province, The Affiliated Hospital of Southwest Medical University, Luzhou 646000, China

[c] Key Laboratory of the Ministry of Education for Medical Electrophysiology, Southwest Medical University, Luzhou, 646000, China

[d] School of Pharmacy, Southwest Medical University, Luzhou 646000,China

[e] Department of Pharmacy, The Affiliated Hospital of Southwest Medical University, Luzhou 646000, China

Highlights

- During its extrahepatic metabolism 4-OHA is reduced by aldo-keto reductases (AKR1C1-AKR1C3) with 3α-, 3β-, and 17β-hydroxysteroid dehydrogenase activities.
- The OH-group attached to C4 of steroids inhibits the reduction of the $\Delta^{4,5}$ double bond by SRD5A1 and SRD5A2. It is responsible for the ability of AKR1C isoforms to catalyse conversion of 4-OHA to metabolites without a $\Delta^{4,5}$ double bond.
- Steroidal aromatase inactivators can be metabolized in the tumour and surrounding tissues, leading to different steroids with different biological anti-tumour properties.

Abstract:

The clinical use of the steroidal aromatase inhibitor Formestane (4-hydroxandrostenedione, 4-OHA) in the treatment of advanced ER+ breast cancer has been discontinued, and therefore, interest in this remarkable drug has vanished. As a C-19 sterol, 4-OHA can undergo extensive intracellular metabolism depending on the expression of specific enzymes in the corresponding cells. We used the metabolites 4β-hydroxyandrosterone, 4β-hydroxyepiandrosterone and its 17β-reduced derivative as standards for the proof of catalytic activity present in the cell culture medium and expressed by the isolated enzymes. All of the aldo-keto reductases AKR1C1, AKR1C2, AKR1C3 and AKR1C4 catalysed the reduction of the 3-keto-group and the $\Delta^{4,5}$ double bond of 4-OHA at the same time. Molecular docking experiments using microscale thermophoresis and the examination of the kinetic behaviour of the isolated enzymes with the substrate 4-OHA proved that AKR1C3 had the highest affinity for the substrate, whereas AKR1C1 was the most efficient enzyme. Both enzymes (AKR1C1and AKR1C3) are highly expressed in adipose tissue and lungs, exhibiting 3β-HSD activity. The possibility that 4-OHA generates biologically active derivatives such as the androgen 4-hydroxytestosterone or some 17β-hydroxy derivatives of the 5α-reduced metabolites may reawaken interest in Formestane, provided that a suitable method of administration can be developed, avoiding oral or intramuscular depot-injection administration.

Keywords: Formestane, Aldo-keto reductase, 3α-HSD, 5α-reductase, Steroid metabolism, Breast cancer

1. Introduction

The steroidal aromatase inhibitor Formestane (4-hydroxandrostenedione, 4-OHA) often shows antiproliferative effects on oestrogen receptor positive (ER+) breast cancers when oestrogen deprivation caused by nonsteroidal aromatase inhibitors such as letrozole or anastrozole fails [1-2]. We have observed that daily topical application of 4-OHA to a female ER+ breast cancer patient can cause a considerable reduction of the size of the tumor within 4 to 6 weeks. This beneficial effect is independent of the prevailing plasma level of oestradiol and is not due to local inhibition of aromatase alone [3].The aromatase-independent mode of action most likely is based on biological effects of metabolites of 4-OHA. Therefore, we wanted to characterize the cellular metabolism of 4-OHA and evaluate which enzyme is primarily involved.

4-OHA is a $\Delta^{4,5}$ keto-steroid. The first and rate-limiting step in the metabolism of such androgens is the reduction of the double bond, catalysed by either 5α- or 5β-reductase. The majority of metabolites present in the urine after oral administration of 4-OHA are 5α-reduced. Therefore, we wanted to determine whether 4-OHA is a substrate for 5α-reductase. Since the metabolism of 4-OHA in the male rhesus monkey proceeds twice as fast as that of its counterpart 4-androstenedione (AD) [4], we anticipated that the obstacle of 5α-reductase is circumvented. To prove this, we expressed recombinant SRD5A1 and SRD5A2 (two distinct isoforms of 5α-reductase) in COS-1 cells and examined the ability of these enzymes to catalyse 5α-reduction of Formestane. Bypassing 5α-reductase could lead to the formation of metabolites of 4-OHA much faster and in many different tissues that do not express 5α-reductase [5]. Our results showed that 5α-reductase did not contribute to the metabolism of 4-OHA.

Since four human aldo-keto reductases (AKR1C1-AKR1C4, AKR1Cs) are well known to play an important role in the intracellular metabolism of steroids, often leading to new molecules exhibiting new biological effects (intracrinology) [6], we used transiently expressed AKR1Cs as well as their isolated counterparts in order to investigate the activities of the corresponding enzymes in the metabolic pathways of 4-OHA and its metabolite 4-hydroxytestosterone (4-OHT), which binds with high affinity to the androgen receptor[37]. In ER+ breast cancers, the metabolites of 4-OHA could have antiproliferative and pro-apoptotic properties.

2. Materials and Methods

2.1 Chemicals and solvents

4-OHA was purchased from Thinker Chemical (Hangzhou, China). Dutasteride was bought from Aladdin (Shanghai, China). 4-hydroxytestosterone (4-OHT) was supplied by Chiracon GmbH company (06-10-1-19P2954), produced and purified as described previously [7]. AD, dihydrotestosterone (DHT), androsterone (ADT) and 3β-androstanediol (3β-diol) were obtained from Yuan Ye (Shanghai, China). 5α-androstanedione (5α-A) was bought from BioBioPha (Kunming, China). Epiandrosterone (EPI) was purchased from Target Molecule Corp. Methyltestosterone (MT) was obtained from Meilunbio (Dalian, China). Flufenamic acid, phenolphthalein, and N-methyl-N-trimethylsilyl-trifluoroacetamide (MSTFA)

were purchased from Sigma. Testosterone (T) was obtained from Cambridge Isotope Laboratories, Inc. NADPH-Na_4 and NADP-Na_2 were from BioFROXX. Other reagents and solvents such as t-butyl methyl ether (MTBE) and dimethylsulfoxide (DMSO) were bought from Merck (Darmstadt, Germany). All other reagents were of American Chemical Society grade or better.

2.1.1 Synthesis of 3β,4β-dihydroxy-5α-androstan-17-one (M2)

5α-androst-3-en-17-one (675 mg, 2.5 mmol, 1.0 eq.) was dissolved into 40 ml acetic acid, followed by the addition of 1.27 g I_2 (5.0 mmol, 2.0 eq.) and 1.1 g $Cu(OAc)_2$ (5.5 mmol, 2.2 eq.). The mixture was stirred and refluxed for about 7 hours and, according to the TLC plate, the starting material was consumed. After cooling down to room temperature, 150 ml of a saturated sodium bisulfite solution were added to the mixture and stirred for another 10 min, and the suspension was filtered through a celite pad. The mixture was four times extracted with DCM (50 ml). The organic phase was combined and dried by $MgSO_4$. Then the solution was removed under reduced pressure to give the crude product. This was recrystallized from acetonitrile and dried in a vacuum oven to yield the fine product M2 as white solid powder. The yield was 560 mg, 73.7%.^{1}H NMR (600 MHz, CD_3OD) 0.77 (3H, s, CH_3-18), 1.23 (3H, S, CH_3-19),3.51 (1H, m, H-3), 3.73 (1H, d, H-4). 1H NMR data was consistent with related reference [8].

2.1.2. Synthesis of 3α,4β-dihydroxy-5α-androstan-17-one (M3)

5α-androst-3-en-17-one (675 mg, 2.5 mmol) was dissolved into 20 ml of 90% formic acid, followed by the addition of 30% hydrogen peroxide (0.5 ml, 5 mmol) at room temperature. The solution was stirred for about 2 hours. Thereafter 5α-androst-3-en-17-one was consumed completely according to the TLC plate. The mixture was diluted with methanol (100 ml) and then basified with 10% aq. sodium hydroxide (pH 10). The mixture was stirred for about 30 min, and was then neutralized with 10% aq. HCl. The solution was extracted three times with dichloromethane and the organic part was combined and washed with st. aq. $NaHCO_3$, filtered and dried with $MgSO_4$. The solution was removed under reduced pressure, the crude product was purified by Si-gel chromatography to give the fine compound M3 700.6 mg, yield89.6%.^{1}H NMR (600 MHz, CD_3OD) 0.88 (3H, s, CH_3-18), 1.08 (3H, S, CH_3-19), 3.53 (1H, s, H-3), 3.79 (1H, d, H-4). 1H NMR data was consistent with related reference [9].

2.1.3. Synthesis of 5α-androstane-3β,4β,17β-triol (Triol)

5α-androst-3-en-17β-yl acetate (791.2 mg, 2.5 mmol, 1.0 eq.) was dissolved into 40 ml acetic acid, followed by the addition of 1.27 g I_2 (5.0 mmol, 2.0 eq.) and 1.1 g $Cu(OAc)_2$ (5.5 mmol, 2.2 eq.). The mixture was stirred and refluxed for about 7 hours and the starting material was consumed over according to the TLC plate. After cooling down to room temperature the suspension was filtered through a celite pad. 150 ml of a saturated sodium bisulfite solution were added to the mixture and stirred for another 10 min. The mixture was extracted by DCM 50 ml for four times. The organic phase was combined and dried by $MgSO_4$, then the solution was removed under reduced pressure to give crude intermediate. The intermediate was dissolved in 20 ml EtOH and treated with 5 ml 15% aq. NaOH solution for about 3 hours. When the intermediate was consumed 40 ml water were added and the pH value was adjusted to 5 with 5% aq. HCl. The mixture was extracted with ethyl acetate 30 ml for four times. The organic phase was combined and dried by $MgSO_4$, the solvent was removed under reduced pressure to give oil residue. The residue was purified by Si-gel chromatography to give desired target Triol as white solid powder 346.1 mg,

yield 44.9%. ^{1}H NMR (600 MHz, CD_3OD) 0.74 (3H, s, CH_3-18), 1.04 (3H, S, CH_3-19), 3.47-3.51 (1H, m, H-3), 3.54-3.59 (1H, t, *J* = 18, 12 Hz, H-17), 3.67 (1H, t, H-4). 1H NMR data was consistent with related reference [10].

2.1.4 Synthesis of 5α-androstane-3α,17β-diol (3α-diol)

5α-androstane-3α-ol-17-one (871.32 mg, 3 mmol) was dissolved into 10 ml methanol and cooled to 0 ^{o}C, sodium borohydride (170.42 mg, 4.5 mmol) was added slowly. The mixture was stirred for a while and allowed to reach room temperature until 5α-androstane-3α-ol-17-one was consumed completely. Water (100 ml) was added to the mixture and the mixture was extracted with ethyl acetate (30 ml) for three times, the organic part was combined and dried with $MgSO_4$, after filtration, the solvent was removed under reduced pressure to give the crude product; Then the crude product was recrystallized from methanol to give the desired fine 3α-diol as white solid powder 694.4 mg, yield 79.1%.^{1}H NMR (600 MHz, CD_3OD) 0.73 (3H, s, 18-CH_3), 0.79 (3H, s, 19-CH_3), 3.61-3.65 (1H, t, H-17), 4.04 (1H, t, H-3).1H NMR data was consistent with related references [11-13].

2.2 Transient transfection of recombinant SRD5A1, SRD5A2 and AKR1Cs in COS-1 cells

Coding sequences of SRD5A1, SRD5A2 and AKR1Cs were synthesized by Sangon Biotech according to GenBank database (*SRD5A1*, AK313070.1; *SRD5A2*, NM_000348.3; *AKR1C1*, NM_001353.5; *AKR1C2,* NM_001354.5; *AKR1C3,* NM_003739.5; and *AKR1C4*, NM_001818.3). All of these genes were constructed in the pcDNA3.1 (+) vector, forming recombinant plasmids pcDNA3.1-SRD5A1, pcDNA3.1-SRD5A2, pcDNA3.1-AKR1C1, pcDNA3.1-AKR1C2, pcDNA3.1-AKR1C3, and pcDNA3.1-AKR1C4, respectively.

Since COS-1 cells (monkey kidney fibroblast cells) do not express or have low expression of AKR1Cs, SRD5A1 and SRD5A2 [14-15], it is considered to be a useful model for studying the function of these enzymes. COS-1-cells were purchased from American Type Culture Collection (Manassas, VA), plated in six-well plates (2.5×10^5 cells/well), and maintained at 37°C and 5% CO_2 in DMEM (GIBCO-11995065) supplemented with 100 U/m penicillin, 100 μg/ml streptomycin, 2 mm L-glutamine, and 10% FBS. After incubation for 24h, COS-1 cells were transfected with 1μg of recombinant plasmid DNA per well. Cells were transfected using Lipofectamine™ 3000 Transfection Reagent (Thermo L3000001) according to the manufacturer's protocol, and all controls were transfected with the pcDNA3.1 (+) vector. The medium was changed 6 h after transfection. In each of these constructs, enzyme expression is driven by the pCMV promoter. The cells were harvested 48h after transfection and analysed by western blot and qPCR. If the enzymes were overexpressed, they could be incubated with substrates or with/without inhibitors.

2.3 Cloning, expression and purification of recombinant AKR1Cs in *Escherichia coli*（*E. coli*）

Similarly, we constructed the synthesized coding sequences of the AKR1Cs into the pET-28a vector with an N-terminal His-tag, forming recombinant plasmids pET28a-AKR1C1, pET28a-AKR1C2, pET28a-AKR1C3, and pET28a-AKR1C4. After transformation with these recombinant plasmids, *E. coli* BL21(DE3) host cells overexpressed recombinant AKR1Cs. The recombinant proteins were purified on a Ni-NTA agarose resin column. The purity of the enzymes was analysed by SDS-PAGE with Coomassie

blue staining, and the protein concentration was determined by an Enhanced BCA Protein Assay Kit (Beyotime P0010S).

2.4 Quantitative real-time PCR (qPCR) analyses of recombinant SRD5A1, SRD5A2 and AKR1Cs in COS-1 cells

After transfection for 48h, total RNA was extracted from the transfected and mock-transfected COS-1 cells with TRIzol (Life Technologies, Inc., Gaithersburg, MD). The first strand cDNA was synthesised according to the PrimeScript™ RT reagent Kit with gDNA Eraser (TaKaRa RR047A). QPCR amplification with TB Green™ IIPremix Ex Taq™ polymerase (TaKaRa RR820A) was performed according to the manufacturer's protocols. β-tubulin(GenBank accession number: XM_007973204.1) was also amplified from the same samples to serve as an internal control. Primers used to detect the expression of recombinant SRD5A1, SRD5A2 and AKR1Cs are listed in Supplementary Table 1.

2.5 Western blot analyses of recombinant SRD5A1, SRD5A2 and AKR1Cs

After transfection for 48h, total protein was extracted from the lysate of the transfected and mock-transfected COS-1 cells using cell lysis buffer without protein denaturant (Beyotime P0013J) supplemented with protease inhibitors of 1% PMSF and cocktail. After purification from *E.coli*, the recombinant AKR1Cs enzymes were diluted for western blot analyses.

Protein concentration was determined by the Enhanced BCA Protein Assay Kit (Beyotime P0010S). Equal amounts of proteins (40μg) were loaded and separated on 10% SDS-PAGE, and transferred to PVDF membranes. The membranes were incubated at 4°C overnight with primary antibodies at a dilution in T-BST containing 5% non-fat dry milk of 1 μg/ml for SRD5A1 (polyclonal antibody, SAB1401372, Sigma-Aldrich), 1:2,000 for SRD5A2 (monoclonal antibody, Abcam, ab124877), 1:1,000 for AKR1C1 and AKR1C2 (polyclonal antibody, CST #13035), 0.5 μg/ml for AKR1C3(monoclonal antibody, R&D system, MAB-7678-SP), and 1:2,000 for AKR1C4 (monoclonal antibody, R&D system, AF6957), repectively, and then for 2h at room temperature with the appropriate anti-IgG horseradish peroxidase (HRP)-conjugated secondary antibody at a dilution of 1:5,000. 1:1,0000 for, β-tubulin was used as the loading control, quantified with a dilution of 1:1,0000 of HRP-Conjugate mouse monoclonal antibody (Zen-bio, 700608).

2.6 Substrate conversion assay by recombinant SRD5A1, SRD5A2 and AKR1Cs in COS-1 cells

After transfecting the cells for 48h, 4-OHA, 4-OHT, AD, T and DHT were added to the medium as substrates dissolved in DMSO at a final concentration of 10 μM with or without 10 μM of the inhibitor and were incubated for 3.5 h. 2 mL of the medium were taken out and added the inner standard MT, and then the sample was extracted after addition of 1.5 mL of K2CO3/KHCO3-solution (20%, 1:1, pH 9.6) with 4 mL of MTBE. The organic layer was separated and evaporated to dryness by nitrogen gas at 40 °C. After derivatization by TMSF, GC-MSMS analysis was performed as described below.

2.7 Substrate conversion assay by purified recombinant AKR1Cs

The reaction system was 200 μL, with 100 mM sodium phosphate buffer (pH 7.4), 5 mM ammonium sulfate, 0.2 mM NADPH-Na_4, 24 μg of enzyme protein of AKR1Cs, and 50 μM of the substrate with or without 100 μM of the inhibitor dissolved in DMSO. The reaction mixtures were maintained at 37°C for 3.5 h and then terminated and extracted by MTBE as the above shown. After derivatization by TMSF, GC-

MSMS analysis was performed as described below.

2.8 Microscale thermophoresis binding assay

The binding affinities of AKR1Cs and 4-OHA were measured using the microscale thermophoresis (MST) method with a NanoTemper monolith NT.115 (US, California). The purified AKR1Cs from the *E. coli* were fluorescently labelled by the Monolith NT^{TM} Protein Labeling Kit (Germany, Munich). 10 mM fluorescently labeled AKR1Cs proteins and 16 serial dilutions of test ligands (ranging from 62.5mM to 0.0153 mM) were respectively co-incubated for 5 min in assay buffer (10 mM KH_2PO_4, 10 mM K_2HPO_4, pH 7.4, 0.2 mM NADPH-Na_4). Then, the samples were loaded into the NanoTemper glass capillaries and microthermophoresis was carried out at a light emitting diode (LED) power of 10% and a MST power of 80%. Quantitative binding parameters are obtained by using the serial dilution. By plotting Fnorm against the logarithm of the different concentrations of the dilution series, a sigmoidal binding curve was obtained. This binding curve can directly be fitted with the nonlinear solution of the law of mass action, with the dissociation constant Kd values, calculated via NanoTemper software from duplicate reads of triplicate experiments.

2.9 Determination of enzyme kinetics

The kinetic constants of reduction were determined in 200 μL systems containing 100 mM sodium phosphate buffer (pH 7.4), with 5 mM ammonium sulfate, 200 μM NADPH-Na_4, and 12 μg AKR1Cs enzymes, respectively. The concentration of the substrates ranged between 2 and 400 μM. All of the enzymatic reactions were followed at 37°C for 30 min. The initial velocities for the reduction of substrates by AKR1Cs were determined by measuring the change of the emission of NADP+ fluorescence derivative stimulated by NaOH at 460 nm with excitation at 360 nm after the reactions were terminated by HCl and the left NADPH was removed simultaneously [16]. The detection method of the kinetic constants of oxidation was the same with reduction except for changing NADPH-Na_4 to NADP-Na_2 and calculating the reduction of NADP+. K_m and V_{max} were determined by the endpoint assay.

2.10 Identification of metabolites by GC-MSMS

Samples (2 mL cell culture medium, 200 μL purified enzyme reaction system) were added 10 ng MT as an internal standard substance, adjusted to pH 9.0 with the addition of carbonate buffer (pH 9.6). The samples were extracted by liquid-liquid extraction with MTBE (4 mL); the mixture was shaken mechanically for 10 min and subsequently centrifuged (1500 g) for 5 min [17]. The organic layer was transferred to a fresh glass tube and evaporated to dryness under nitrogen gas at 40 °C. The dry residue was derivatized with 50 μL of MSTFA/NH4I/dithioerythritol (1000:2:4, v/w/w), which is equivalent to a mixture of MSTFA/trimethyl iodo silane (TMS) and heated for 20 min at 60 °C. Trimethylsilyl (TMS)-enol and TMS-ethers were formed [8].

The GC-MSMS analyses were performed on an Agilent 7890A gas chromatograph coupled to an Agilent 7000 triple quadrupole mass spectrometer (Agilent Technologies SpA, Cernuscosul Naviglio, Milano, Italy). The injector line operated at 280 °C and the transfer line at 300 °C. The initial temperature of 177 °C was increased at 3 °C/min to 245 °C and then increased at 17 °C/min to 320 °C and kept for 3.2 min at the final temperature. The injection volume was 2 μL in split mode (1:3) [17-18]. Helium was used

as the carrier gas (1.5mL/min).The products were qualified by their retention times under specific MRM mode [8, 18] as described in supplementary Table 2, and the ion chromatograms are shown in supplementary Fig. 1. They were quantified by standard curves from continuous contents of standard substances.

2.11 Statistical analysis

All experiments were performed in triplicates and the results are presented as the means ± SEM. Statistical significance was determined by Student's *t*-test, and V_{max} and K_m values were calculated according to the Michaelis-Menten equation and a nonlinear regression curve, using GraphPad Prism version 5 (GraphPad Software, San Diego, CA, USA). Histograms of two dimensions with metabolite content ratio were drawn by GALLERY, an open source software from https://gallery.echartsjs.com.

3 Results

3.1 Cloning, expression and purification of enzymes

After the recombinant plasmids pcDNA3.1-SRD5A1, pcDNA3.1-SRD5A2, pcDNA3.1-AKR1C1, pcDNA3.1-AKR1C2, pcDNA3.1-AKR1C3, and pcDNA3.1-AKR1C4 were transiently transfected into COS-1 cells, qPCR results showed that the SDR5A- and AKR1C- enzymes were overexpressed, compared with endogenous highly-expressed β-tubulin (Fig.1A). Furthermore, the proteins of the AKR1C enzymes and the SRD5A enzymes were successfully transiently overexpressed in COS-1 cells, according to the western blot result (Fig.1C upper and middle panel). Therefore, from both transcription- and protein levels of the enzymes, it was concluded that this cell system could be used for identification of the metabolites of 4-OHA and 4-OHT originating from reactions catalysed by SRD5A1, SRD5A2 and AKR1Cs.

After the recombinant plasmids pET28a-AKR1C1, pET28a-AKR1C2, pET28a-AKR1C3, and pET28a-AKR1C4 were transfected into *E. coli* BL21 (DE3), each AKR1Cs' elution, flow-through and the soluble supernatant of the lysate were used for SDS-PAGE analyses. All four enzymes were present in the supernatant exhibiting a molecular weight of 37KD and were eluted with 90% purity (Fig. 1B). Furthermore, the western blot also showed that the recombinant AKR1C proteins were expressed in COS-1 and in E.coli (Fig. 1C lower panel). Therefore, all of the AKR1C proteins from *E. coli* could be used for catalytic reactions, molecular docking and kinetic analyses.

3.2 Analyses of the reaction products obtained in COS-1 cells after transfection with SRD5A1 and SRD5A2

The incubation of AD and T with the medium of the COS-1 cells transfected with SRD5A1 and SRD5A2 led to the conversion of AD into 5α-A, some DHT, and a little ADT, EPI, 3α-diol and 3β-adiol, and the conversion of T mostly into of DHT, and a little 3α-diol and 3β-diol (Fig. 2C, D). The conversions were inhibited by Dutasteride. Therefore, SRD5A1 and SRD5A2 were successfully temporarily expressed with 5α-reductase activity in COS-1 cells. The set of experiments also showed that there were some endogenous 3α-HSD, 3β-HSD and 17β-HSD activities in COS-1 cells since some 3α-, 3β- and 17β-hydroxy products such as ADT, EPI, DHT, 3α-diol and 3β-adiol appeared. There was a little endogenous 5α-reductase activity, since small amounts of 5α-reduced metabolites of AD and T were detected in mock-

transfected cells. However, compared with over-expressed recombinant 5α-reductases, this did not influence the results obtained after incubation of 4-OHA and 4-OHT with 5α-reductase.

Neither 4-OHA nor 4-OHT were substrates for the recombinant 5α-reductase, and corresponding metabolites could also not be detected (Fig. 2A, B), which agreed well with previous reports [19]. This suggested that other intracellular sterol metabolizing enzymes are able to reduce the $\Delta^{4,5}$ double-bond of a C-19 steroid with a hydroxyl group attached to C4, a configuration obviously impeding 5α-reduction as judged by the usual method. Indeed almost all urinary metabolites of 4-OHA or 4-OHT after oral administration show 5α-reduction with concomitant or subsequent 3α- or 3β-reduction [8]. The obvious choices were the human cytosolic aldo-keto reductases AKR1C1, AKR1C2, AKR1C3 and AKR1C4.

In contrast to oral administration, intravenous administration to postmenopausal breast cancer patient leads to the appearance of the glucuronide of 4-OHA and of some minor metabolites, but a considerable part of the urinary metabolites are the sulphates of M2 (4β-hydroxy-epiandrosterone) and M3 (4β-hydroxy-androsterone) [20]. "Triol" is the 17β-hydroxy derivative of M2, most likely formed within the cells.

3.3 Binding preference of 4-OHA and 4-OHT to the different AKR1Cs

The above results led to the assumption that other sterol metabolizing enzymes are able to reduce the $\Delta^{4,5}$ double-bond. We therefore performed docking experiments of AKR1Cs to 4-OHA and 4-OHT by MST to get Kd values, directly reflecting their interaction.

Both 4-OHA and 4-OHT bound to all AKR1Cs yielding different Kd values (Fig.3). AKR1C3 had the lowest Kd at 6.7 nM, followed by AKR1C1 and AKR1C4, and AKRIC2 had the highest Kd at 47.1 nM (Fig.3 A-D). Hence, the binding affinity of 4-OHA with AKR1C3 was the highest. The affinity of AKR1C2 for the steroid was considerably lower. Also to 4-OHT, AKR1C3 had the lowest Kd at 14.8nM. AKR1C2 had the highest Kd at 57.4 nM. 4-OHT had somewhat lower binding affinities to all AKR1Cs than 4-OHA (Fig.3 E-H), which suggested that the presence of a keto-group at C17 instead of a β-OH-group favours binding to the AKR1Cs.

3.4 Reaction product analysed after incubation with recombinant AKR1Cs from COS-1cells

To determine which of the major AKR1C enzymes is involved in the metabolism of 4-OHA and 4-OHT, the assessment of the directionality of AKR1Cs in a cellular environment was investigated. The metabolisms of AD, T, and DHT served as controls. When mock transfected COS-1 cells were incubated with AD, it was converted to T, incubation with T gave rise to AD, 3α-diol and 3β-diol; and incubation with DHT led to the appearance of 3α-diol and 3β-diol, apparently due to endogenous 3α-HSD, 3β-HSD and 17β-HSD activities (Fig. 4C-E). However, the endogenous HSD activities did not affect the examination of the functions of the transfected AKR1Cs since these had much higher activities than the endogenous HSDs. For example, DHT is easily reduced by 3alpha/beta-HSD and in mock-transfected cells 60% of DHT is converted into 3alpha-diol and 3beta-diol. In AKR1Cs-transfected cells, however, at least 80% of DHT is reduced. Most efficient were AKR1C2 and AKR1C4-transfected cells. Nearly 100% of DHT is reduced to the diols (Fig.4D).

The metabolism of AD in COS-1 cells transfected with the different AKR1Cs showed that only AKR1C3 had obvious reductive 17beta-HSD activity (Fig. 4C). The metabolism of DHT showed that all

AKR1Cs had both 3α- and 3β-HSD activities, AKR1C2 and AKR1C4 had a higher 3α-HSD activity, whereas AKR1C1 and AKR1C3 had a higher 3β-HSD activity (Fig. 4D). There was some slight oxidation of T by AKR1C1 and AKR1C3 to AD. That of 4-OHT to 4-OHA was considerably more pronounced. In the medium of COS-1 cells transfected with AKR1C2 or AKR1C4, diol formation was observed (and most likely due to endogenous enzyme activity within the cells?) (Fig. 4E). The above results are consistent with several related studies [21-23], suggesting that our recombinant enzyme reaction systems in COS-1 cells were suitable to study the metabolism of 4-OHA and 4-OHT.

Since after intravenous injection of a small amount of ^{14}C-labelled 4-OHA, the major metabolites found in the urine of postmenopausal breast cancer patients are reduced at C3 and preferentially conjugated with a sulphate group (M2 and M3 exist exclusively as sulphates) [20], we put emphasis on the ability of the enzymes to catalyse the 3β-reduction that would lead to M2. It is obvious that the extrahepatic formation of this metabolite could be catalysed by AKR1C1 and AKR1C3 and not by AKR1C2 and AKR1C4 (Fig. 4A). AKR1C4, which is expressed in the liver only, but not AKR1C2, had a higher capacity to metabolize 4-OHA and the product was mainly M3, the 3α-hydroxy-isomer of M2. Triol was most likely the result of the interaction of M2 with AKR1C3. Our results demonstrated that all AKR1Cs could reduce the 4-5 double bond since M2 and M3 are 5α-androstanes. This corresponds to the urinary steroid profile after oral ingestion of 4-OHA [8].

Furthermore, all AKR1Cs had 17β-HSD activity and converted 4-OHA to 4-OHT, which was most obvious for AKR1C3 and AKR1C4. The 17β-HSD activity also led to Triol, the presumable metabolite of 4-OHA and 4-OHT. Overall, 4-OHA was metabolized by all AKR1Cs, and the rank order of metabolic activity towards 4-OHA was AKR1C4>AKR1C3>AKR1C1>AKR1C2. All AKR1Cs catalysed the conversion of 4-OHT to 4-OHA, M3 and Triol, demonstrating 17-oxidase, 4-5 double bond reductase, and 3α/β-HSD activities of these enzymes (Fig. 4B).

3.5 Analyses of the reaction products of 4-OHA and 4-OHT after incubation with recombinant AKR1Cs purified from *E. coli*

For consolidating and extending the study of the role of AKR1Cs in the metabolism of 4-OHA and 4-OHT, we further incubated the isolated recombinant AKR1Cs from *E.coli* with NADPH and the substrates under investigation in order to detect and quantify the metabolites by GC-MSMS.

For AD, all isolated AKR1Cs reduced AD to T presenting 17-keto reductase activity. AKR1C3 was most active as a 17-ketosteroid reductase followed by AKR1C1and then AKR1C2, whereas AKR1C4 only weakly reduced AD to T (Fig. 5C). For DHT, all four enzymes exhibited both 3α/β-keto-reductase activities to various degrees. The major sources of 3β-diol were AKR1C1, AKR1C3, and AKR1C4, and that of 3α-diol was AKR1C2 (Fig.5D). In this set-up, isolated AKR1C4 preferentially catalysed the 3β-reduction of DHT. Interestingly, inhibition by phenolphthalein changed the stereoselectivity back to the normal 3α-reduction. For T, AKR1Cs had no catalytic function and even no oxidative 17β-HSD activity (Fig.5E). These results indicated that the purified recombinant AKR1Cs showed own intrinsic enzyme activities and the reactions of the androgens AD, T to ADT or EPI could only be catalysed by all AKR1Cs after classical 5α-reduction.

For 4-OHA, some AKR1Cs behaved as 17β-HSD or as 3β-HSD, but all AKR1Cs converted 4-OHA to M3, possibly reducing the keto-group at C4, thereby eliminating the double bond to varying extent. AKR1C3 was most active as a 17-ketosteroid reductase and was inhibited by flufenamic acid. AKR1C4 showed higher activities of 4-keto-reductase, 3α-HSD, and 3β-HSD, producing the largest amount of M3 and M2, which was strongly inhibited by phenolphthalein. The rank order of possible metabolic activities towards 4-OHA was AKR1C3>AKR1C4>AKR1C1>AKR1C2 (Fig.5A). This was in stark contrast to the conditions found for the metabolism of DHT. In contrast to the SRD5A1-catalysed metabolism of AD in the rhesus monkey the metabolism of the 4-hydroxy derivative apparently has no such bottle neck and proceeds twice as fast [4].

Like testosterone 4-OHT is not a good substrate for AKR1C1 and AKR1C2. In contrast to T 4-OHT undergoes some AKR1C catalysed metabolism. Both AKR1C3 and AKR1C4 had some oxidative 17β-HSD activity, and AKR1C4 has additional obvious 4-5 double bond reductase and 3-keto reductase activities, making a good production of M3 (Fig. 5B). AKR1C3 predominantly catalysed the reduction at C17 of AD as a first step, whereas it catalysed the first step in the metabolism of 4-OHT as oxidative 17β-HSD, which we have not investigated before. Apparently, AKR1C4 also catalysed the way of 4-OHT via a special 17β-hydroxy pathway to 3α-adiol, a pathway whereby the 17β OH-group is preserved. This has been described for the metabolism of testosterone [20]. AKR1C4 showed obvious 4-5 double bond reductase and 3-keto reductase activities, producing M3 and some Triol, and it was almost entirely inhibited by phenolphthalein. Flufenamic acid inhibited the 3α-HSD and 3β-HSD activities of all AKR1Cs.

3.6 **Steady-state kinetic analyses**

The determination of enzyme kinetic parameters such as Km, Vmax, Kcat and Kcat/Km for the reduction of 4-OHA, 4-OHT and their controls (DHT, AD, and T) showed that the parameters for a given sterol were different depending on the enzymes (Table 1). T was not metabolized by all AKR1Cs, AD was only reduced by AKR1C3, and DHT was reduced by all AKR1Cs. In addition, oxidation of androsterone (ADT) by AKR1Cs was determined, indicating that ADT was oxidized by AKR1C1, AKR1C2 and AKR1C4, and was not oxidized by AKR1C3 (Supplementary Table 3). Taken together, the characteristics of their affinity and reaction efficiency were nearly consistent with reference 21, confirming that these enzymes had the desired activity and that a functioning reaction system was available.

For 4-OHA, the rank order of K_m for the different AKR1Cs was AKR1C3<AKR1C1<AKR1C4<AKR1C2, suggesting that 4-OHA had the highest affinity to AKR1C3 then to AKR1C1 and AKR1C4, and exhibits the lowest affinity to AKR1C2. However, judged from Vmax and Kcat values, AKR1C2 possesses the highest catalytic rate and the lowest is found with AKR1C3.The K_{cat}/K_m value represents the catalytic efficiency of an enzyme. Its values for 4-OHA were AKR1C1>AKR1C3>AKR1C4>AKR1C2, which means that the catalytic efficiency of AKR1C1 is higher than that of AKR1C3. These results are consistent with the binding preferences of 4-OHA to AKR1Cs established by MST. 4-OHT has a high affinity for AKR1C4 and AKR1C1, then comes AKR1C2, and there was no affinity of 4-OHT shown for AKR1C3, which was similar to the reaction efficiency. The affinities of the AKR1Cs for 4-OHT were lower than for 4-OHA, and the reaction efficiency of the AKR1C enzymes in the metabolism of 4-OHA was much higher than that of 4-OHT.

Discussion

The steroids 4-OHA and 4-OHT are selective inhibitors of aromatase [25] not only inhibiting the enzyme but inactivating it (mechanism-based inhibitors). 4-OHA has been used successfully in metastatic breast cancer after failure of tamoxifen [26]. The clinical usefulness of transdermal 4-OHT in the metastatic setting is currently under investigation [27]. Because extensive hepatic metabolism and conjugation of 4-OHA after oral administration lead to a low bioavailability, an injectable drug was developed, where a single dose contained 250 mg of lyophilized 4-OHA and a fluid for reconstitution before intramuscular injection (Lentaron®i.m. Depot). This depot injection was given every two weeks.

In this study, we demonstrated that 4-OHA and 4-OHT were not the substrates for SRD5A1 and SRD5A2 transiently expressed in COS-1 cells, and furthermore that the reduction of their $\Delta^{4,5}$ double bond was catalysed by transiently expressed human cytosolic aldo-keto reductases AKR1C1-AKR1C4. AKR1C1 and AKR1C3 were the most active enzymes in the extrahepatic metabolism of 4-OHA.

After oral ingestion by male volunteers the majority of urinary metabolites were 5α-reduced and glucuronidated [8]. Of the urinary metabolites after oral ingestion only M2 is exclusively sulphated [8]. The hepatic metabolism of 4-OHA and 4-OHT involves all four AKR1C enzymes, which are expressed in the liver to a similar extent [22]. AKR1C4 is only expressed in the liver. After an intravenous pulse dose of 1 mg of ^{14}C-labelled 4-OHA in postmenopausal breast cancer patients who had previously received fortnightly five i.m doses (250 mg) of Lentaron-Depot, urinary radioactivity showed an almost exclusive association with two major sulphated metabolites and the glucuronide of 4-OHA. The sulphated metabolites are M2 and M3, appearing in the urine in a ratio of 7:3 [20]. The predominance of sulphated metabolites and the preponderance of the 3β-OH metabolite came as a surprise. Our results contribute to the explanation of this phenomenon by showing that AKR1C1 exhibits preferential 3β-reduction and AKR1C3 is not a very active 3α- or 3β-HSD. Both enzymes are responsible for the extrahepatic metabolism of 4-OHA. The fact that there are not many glucuronides found in the urine of these patients except the glucuronide of the unchanged drug indicates that after i.v. injection the metabolism of the drug occurs to a considerable part extrahepatically. This most likely is also the case for the drug reaching the bloodstream after the depot injections used in the clinic. Since 4-OHA undergoes some metabolism in extrahepatic tissues and also in the tumour, which gives rise to active substances, this may explain its effectiveness in cases where previous oestrogen deprivation by nonsteroidal aromatase inhibitors has failed.

The hydroxyl group at C4 apparently prevents the activity of 5α-reductases but allows the elimination of the $\Delta^{4,5}$ double bond. The responsible AKR1C enzyme probably first reduces the 4-keto group that is a short-lived constituent of the keto-enol tautomerism and then reduces the keto-group at C3. In the metabolism of 4-OHA, the hydroxyl group at C4 persists.

There are two other 4-OH-steroids closely related to 4-OHA and 4-OHT. These are the anabolic substances oxymesterone (4-OHT with a 17α methyl-group) and oxabolone (4-OHT without C19). There are differences in the metabolism of these two anabolic androgenic steroids and that of 4-OHA. Oxymesterone gives rise to 5α-reduced metabolites with a 4-keto group [17], and in oxabolone the 3-keto group may persist after reduction of the double bond [26]. The mechanism of 5α-reduction of 4-hydroxy steroids by cytosolic aldo-keto reductases are still obscure.

The possibility to bypass 5α-reductase apparently increases the speed of the metabolism of 4-OHA and 4-OHT. In the male rhesus monkey, the metabolic clearance rate (MCR) of intravenously injected AD is only 40% of that of injected 4-OHA [5]. The MCR of AD in postmenopausal women is 1200 L/24 h [30] and that of 4-OHA is approximately 6000 L/24 h [19]. The greater MCR of 4-OHA is probably due to the fact that AKR1C1 and AKR1C3 have a wider tissue distribution than 5α-reductase. The most important tissues in this respect are probably adipose tissue and the lung. AKR1C3 is highly expressed in lung, breast and prostate gland [22] as well as in adipose tissue [30]. The activity of 5α-reductase in the lung is very low [31]. In subcutaneous adipose tissue, the expression of AKR1C3 is 30 times higher than that of 5α-reductases and the expression of AKR1C1 is 70 times higher [30]. This is an important aspect for transdermal delivery of 4-OHA to the blood and the tumour.

After injection of DHT in rats, the majority of the radioactivity can already be found after only three minutes in the 3α-diol fraction. This quick metabolism is independent of the liver or kidney [32].The likely organ of DHT-metabolism in the rat is the lung because 98% of the blood returning from the body to the right atrium is bound to pass through the capillaries of the lung and every substance present in the venous blood leaving the liver also has to pass through the lung. It has been shown that 100 mg of homogenized lung tissue from adult male rats consumes 90% of the ^{3}H-DHT. The capacity of the lung of the rat sufficiently explains the rapid disappearance of DHT from the blood [33]. Intravenously or parenterally administered substances can be metabolized by the lung, provided the necessary enzymes are expressed in this organ. AKR1C1 and AKR1C3 are highly expressed in this organ [22]. The lung may play an important role in the metabolism of 4-OHA.

In postmenopausal women, adipose tissue is a major source of oestrogens in the blood [34-35]. Nonsteroidal aromatase inhibitors such as anastrozole or letrozole can lower systemic levels of E2 by 90%. [36], whereas the effect of 4-OHA is much weaker. Nevertheless, Formestane can induce disease stabilization in postmenopausal advanced breast cancer patients progressing on letrozole, anastrozole, and aminoglutethimide. This effect is completely independent of the E2 level, which usually increases after withdrawal of nonsteroidal aromatase inhibitors [3]. The inability of 4-OHA to lower systemic levels of E2 sufficiently in comparison with nonsteroidal aromatase inhibitors may be due to the rapid change of structure of the aromatase-inactivator 4-OHA in adipose tissue. The clinical effectivity of 4-OHA may be due in a considerable part to the biological effects of locally formed metabolites of 4-OHA.

The most obvious of such steroids is 4-OHT, which has a very high affinity to the androgen receptor (AR) [37]. In the past, the androgen testosterone-propionate (TP) has been successfully used in the treatment of advanced breast cancer [38]. In cultures of ER+ breast cancer cells expressing the AR, androgenic substances can inhibit the proliferation of the cancer cells [39]. AKR1C3 is highly expressed in all types of breast cancer [40], even in cells representative of triple negative breast cancer [41].

The two major sulphated metabolites of intravenously administered 4-OHA are M2 and M3. They are products of the metabolism of 4-OHA catalysed by the AKR1C enzymes. Since the 3β reduction prevails, the most likely active candidate enzymes are AKR1C1 and, according to our results, AKR1C3. Both end products (M2 and M3) can be reduced at C17 by AKR1C3 and become molecules with affinities to nuclear receptors such as AR, ERα and ERβ, etc. It is conceivable that 4-OHT is not the only biologically active

metabolite of 4-OHA. A major candidate is Triol (3β,4β,17β-trihydroxy 5α-androstane), a proven in vitro metabolite. Together with 4-OHT this and other not yet evaluated metabolites may contribute to the clinical efficacy of Lentaron-Depot even when oestrogen deprivation cannot inhibit the progression of advanced breast cancer.

Conclusion

All four AKRICs (AKR1C1-AKR1C4) act as reductases for 4-OHA in both COS-1 cells and in reaction systems with purified enzymes. They exert 3α-, 3β-, and 17β-hydroxysteroid dehydrogenase activities and even a newly described catalytic function, 4-5 double bond reduction.

Acknowledgements

This work was supported by start-up funding (Grant numbers 16169, 16248) from the Affiliated Hospital of Southwestern Medical University, Luzhou grants (Grant numbers 02-00040055, 02-00040108), and a Southwestern Medical University grant (Grant number2018-ZRZD-004). We express heartfelt thanks to Sheng Yang from the China Anti-Doping Agency, Tianzhu Zang from the University of Pennsylvania, and Yuanji Gao from the Sichuan Normal University for their technical advice on the identification of metabolites and to Iqra from the Sichuan Provincial Center for Gynaecology and Breast Diseases for serious revision of the manuscript.

Declarations of interest: none.

References

[1] P. Carlini, A. Frassoldati, S. De Marco, A. Casali, E.M. Ruggeri, M. Nardi, P. PapaldoP, A. Fabi, F. Paoloni, F. Cognetti. Formestane, a steroidal aromatase inhibitor after failure of non-steroidal aromatase inhibitors (anastrozole and letrozole):is a clinical benefit still achievable? Ann Oncol. 11(2001) 1539-1543.

[2] P. Carlini, G. Ferretti, S. Di Cosimo, E. Collela, R. Tonachella, A. Romiti, S. Tomao, A. Frassoldati, P. Papaldo, A. Fabi, E.M. Ruggeri, F. Cognetti. Is there a benefit by the sequence anastrozole-Formestane for postmenopausal metastatic breast cancer women? J Steroid BiochemMol Biol. 86 (2003)107-109.

[3] N. Zilembo, E. Bajetta , E. Bichisao, A. Martinetti, I. La Torre, P. Bidoli, R. Longarini R, T. Portale, E. Seregni, E. Bombardieri E. The estrogen suppression after sequential treatment with Formestane in advanced breast cancer patients. Biomed Pharmacother.58 (2004) 255-259.

[4] A.M. Brodie, L.P. Romanoff, K.I. Williams. Metabolism of the aromatase inhibitor 4-hydroxy-4-androstene-3,17-dione by male rhesus monkeys. J Steroid Biochem. 8 (1981) 693-696.

[5] T.M. Penning, M. Chen, Y. Jin. Promiscuity and diversity in 3-ketosteroid reductases. J Steroid BiochemMol Biol. 151 (2015) 93-101.

[6] F. Labrie. At the cutting edge intracrinology. Mol Cell Endocrinol.78 (1991) C113-118.

[7] L.H. Knox, E. Blossey, H. Carpio, L. Cervantes, P. Crabbé, E. Velarde, J.A. Edwards. Steroids.CCLXXVIII.1 Reductions of 19-Substituted Androst-4-en-3-ones and Related Compounds. J. Org. Chem.30 (1965) 2198-2205.

[8] M. Kohler, M.K. Parr, G. Opfermann, M. Thevis, N. Schlörer, F.J Marner, W. Schänzer.Metabolism of 4-hydroxyandrostenedione and 4- hydroxy-testosterone: Mass spectrometric identification of urinary metabolites. Steroids.3 (2007) 278-286.

[9] E.J. Tavares da Silva, M.L. Sá e Melo, A.S. Campos Neves. Novel approach to the synthesis of the aromatase inhibitor 4-hydroxyandrost-4-ene-3,17-dione (4-OHA). J. Chem. Soc., Perkin Trans. 1(1996) 1649-1650.

[10] M.M. Cruz Silva, S. Riva, M. Luisa Sá e Melo. Regioselective enzymatic acylation of vicinal diols of steroids.Tetrahedron61(2005) 3065-3073.

[11] A. Świzdor, A. Panek, N. Milecka-Tronina. Microbial Baeyer–Villiger oxidation of 5α-steroids using Beauveriabassiana. A stereochemical requirement for the 11α-hydroxylation and the lactonization pathway.Steroids82 (2014) 44-52.

[12] N. Kennedy and T. Cohen. The stereoselective reductions of ketones to the most thermodynamically stable alcohols using lithium and hydrated salts of common transition metals. J Org Chem. 80 (2015) 8134-8141

[13] I. Gavrilovic, K. Mitchell, A.D. Brailsford, D. A. Cowan, A.T. Kicman, R.J. Ansell. A molecularly imprinted receptor for separation of testosterone and epitestosterone, based on a steroidal cross-linker. Steroids 76 (2011) 478-483]

[14] T. Lanišnik-Rižner, H.K. Lin, D. M. Peehl, S. Steckelbroeck, D.R. Bauman, T.M. Penning. Human Type 3 3α-Hydroxysteroid Dehydrogenase (Aldo-Keto Reductase 1C2) and Androgen Metabolism in Prostate Cells, Endocrinology, 144 (2003) 2922-2932.

[15] L.N. Thomas, R.C. Douglas, J.P. Vessey, R. Gupta, D. Fontaine, R.W. Norman, I.M. Thompson, DA. Troyer, RS. Rittmaster, CB. Lazier. 5alpha-reductase type 1 immunostaining is enhanced in some prostate cancers compared with benign prostatic hyperplasia epithelium, J Urol.170 (2003) 2019-25.

[16] S.P. Dufrane, W.J. Malaisse, A. Sener. A micromethod for the assay of aldose reductase, its application to pancreatic islets. Biochem Med. 32 (1984) 99-105.

[17] S. Yang, J. Lu, Y. Xu, X. Wang. New oxymesterone metabolites in human by gas chromatography-tandem mass spectrometry and their application for doping control. Drug Test Anal. 7 (2016) 633-643.

[18] A.T.Cawley, G.J.Trout, R.Kazlauskas, A.V.George. The detection of androstenedione abuse in sport: a mass spectrometry strategy to identify the 4−hydroxyandrostenedione metabolite. Rapid Commun.Mass Spectrom. 22(2008) 4147-4157.

[19] H.L. Holland, S. Dore, W. Xu, F.M. Brown. Formation of 5 alpha steroids by biotransformation involving the 5 alpha-reductase activity of Penicillium decumbens.Steroids. 59 (1994) 642-647.

[20] P.E. Lønning, J. Geisler, D.C. Johannessen, H.P. Gschwind, F. Waldmeier, W. Schneider, B. Galli, T. Winkler, W. Blum, H.P. Kriemler, W.R. Miller, J.W. Faigle. Pharmacokinetics and metabolism of Formestane in breast cancer patients. J Steroid Biochem Mol Biol. 77 (2001) 39-47.

[21] S. Steckelbroeck, Y. Jin, S. Gopishetty, B. Oyesanmi, T.M. Penning. Human cytosolic 3alpha-hydroxysteroid dehydrogenases of the aldo-keto reductase superfamily display significant 3beta-hydroxysteroid dehydrogenase activity: implications for steroid hormone metabolism and action. J Biol Chem. 279 (2004) 10784-10795.

[22] T.M. Penning, M.E. Burczynski, J.M. Jez, C.F. Hung, H.K. Lin, H. Ma, M. Moore, N. Palackal, K. Ratnam. Human 3alpha-hydroxysteroid dehydrogenase isoforms (AKR1C1-AKR1C4) of the aldo-keto reductase superfamily: functional plasticity and tissue distribution reveals roles in the inactivation and formation of male and female sex hormones. Biochem J. 351 (2000) 67-77.

[23] T.M. Penning, Y. Jin, S. Steckelbroeck, T. Lanišnik Rižner, M. Lewis: Structure-function of human 3 alpha-hydroxysteroid dehydrogenases: genes and proteins. Mol Cell Endocrinol. 215 (2004) 63-72.

[24] E.E Baulieu, P. Mauvais-Jarvis. Studies on testosterone metabolism. I.Conversion of testosterone-17-alpha-3H to 5-alpha- and 5-beta-androstane-3-alpha,17beta-Diol-17-alpha-3H: A new "17-beta-hydroxyl pathway". J Biol Chem. 239 (1964)69-77.

[25] A.M. Brodie, W.C Schwarzel, H.J. Brodie. Studies on the mechanism of estrogen biosynthesis in the rat ovary-I.J Steroid Biochem. 10 (1976)787-793.

[26] L.R Wiseman, D. McTavish. Formestane. A review of its pharmacodynamic and pharmacokinetic properties and therapeutic potential in the management of breastcancer and prostatic cancer.Drugs. 45 (1993) 66-84.

[27] M. Zweifel, B. Thürlimann, S. Riniker, P. Weder, R. von Moos, O. Pagani, M Bigler, K.M. Rothgiesser,C. Pilop, H.Hawle, C. Brauchli, C. Tapia, W. Schoenfeld, C. Sessa; Swiss Group for Clinical Cancer Research (SAKK). Phase I trial of the androgen receptor modulator CR1447 in breast cancer patients. Endocr Connect. 7 (2017) 549-556.

[28] M.V. Barbarulo, F. Buiarelli, M. Ciardi, A. Giarrusso, A. Giarrusso, R. Cartoni. Capillary GC-MS investigation of the metabolism and excretion of oxabolone in man J High Resolut Chromatogr 8 (1995)705-708.

[29] C. Longcope, W. Jaffee, G. Griffing. Metabolic clearance rates of androgens and oestrogens in ageing women. Maturitas. 4 (1980) 283-290.

[30] K. Blouin, A. Veilleux, V. Luu-The, A. Tchernof. Androgen metabolism in adipose tissue: recent advances. Mol Cell Endocrinol.301(2009) 97-103.

[31] L. Milewich, P.S. Parker, P.C. MacDonald. Testosterone metabolism by human lung tissue. J Steroid Biochem. 1 (1978) 29-32.

[32] V. L. Gay. Ineffectiveness of DHT treatment in producing increased serum DHT in orchidectomized rats. Evidence for rapid in viva metabolism of DHT to androstanediol. Fed.Proc. 34 (1975) 303.

[33] L.W. Kao, M.J. Crosswell, J. Weisz. Steroid metabolism by the lung: conversion of dihydrotestosterone to 5 alpha-androstan-3 alpha, 17 beta-diol by rat lung tissue in vitro. Endocrinology. 104 (1979)664-666.

[34] D.L. Hemsell, J.M. Grodin, P.F Brenner, P.K. Siiteri, P.C. MacDonald. Plasma precursors of estrogen. II. Correlation of the extent of conversion of plasma androstenedione to estrone with age. J ClinEndocrinolMetab. 38 (1974)476-479.

[35] S.E. Bulun, E.R. Simpson. Competitive reverse transcription-polymerase chain reaction analysis indicates that levels of aromatase cytochrome P450 transcripts in adipose tissue of buttocks, thighs, and abdomen of women increase with advancing age. J Clin Endocrinol Metab. 78 (1994) 428-432.

[36] R.C. Coombes. Aromatase inhibitors and their use in the adjuvant setting. Recent Results Cancer Res. 152 (1998)277-84.

[37] J.H. Davies, R.J. Shearer, M.G. Rowlands, G.K. Poon, J. Houghton, M. Jarman, M. Dowsett. Effects of 4-hydroxyandrost-4-ene-3,17-dione and its metabolites on 5alpha-reductase activity and the androgen receptor. J Enzyme Inhib. 6 (1992)141-147.

[38] I.S. Goldenberg. Testosterone propionate therapy in breast cancer. JAMA.188 (1964) 1069-1072.

[39] S.N. Birrell, J.M. Bentel, T.E. Hickey, C. Ricciardelli, M.A. Weger, D.J. Horsfall, W.D.Tilley. Androgens induce divergent proliferative responses in human breast cancer cell lines. J Steroid BiochemMol Biol. 52 (1995) 459-467.

[40] K.M. McNamara, H. Sasano. The role of 17βHSDs in breast tissue and breast cancers.Mol Cell Endocrinol. 18 (2018)30314-30319.

[41] K.M. McNamara, T. Yoda, A.M. Nurani, Y. Shibahara, Y. Miki, L. Wang, Y. Nakamura, K. Suzuki, Y. Yang, E. Abe, H. Hirakawa, T. Suzuki, N. Nemoto, M. Miyashita, K. Tamaki, T. Ishida, K.A. Brown, N. Ohuchi, H. Sasano. Androgenic pathways in the progression of triple-negative breast carcinoma: a comparison between aggressive and non-aggressive subtypes. Breast Cancer Res Treat. 145 (2014) 281-293.

Figure Legends

Fig.1 Transfection into COS-1 cells and successful expression of SRD5A1, SRD5A2 and AKR1Cs. A: Relative expression levels of mRNA of recombinant SRD5A1 and AKR1Cs in transfected COS-1 cells. *β-Tubulin* was set as reference gene. The data is expressed as a histogram containing the means ± SEM. of three independent experiments (n=3 each group).* P<0.05; ** P<0.01. **B:** SDS-PAGE analyses of recombinant AKR1Cs after purification from the lysates of *E. coli* BL21(DE3) .**C:** Western blot analyses of recombinant SRD5A1 and SRD5A2 and of AKR1Cs. pcDNA3.1 served as negative control, and β-Tubulin was used as internal reference.

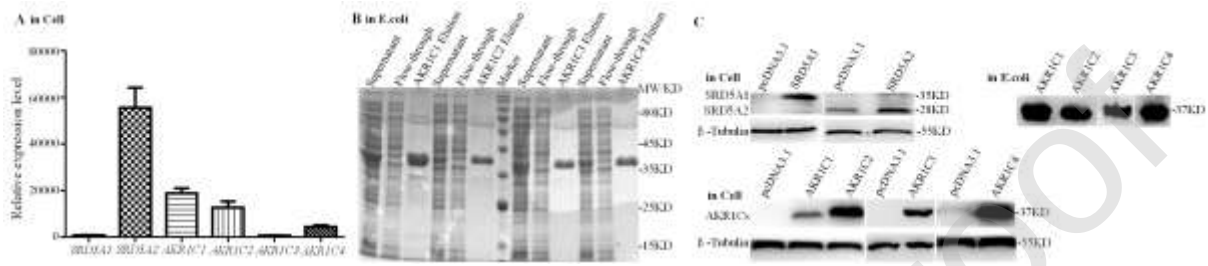

Fig.2 Recovery of metabolites from the medium of COS-1 cells transfected with SRD5A1 and SRD5A2. After transfection of COS-1 cells for 48h with pcDNA3.1-SRD5A1 or pcDNA3.1-SRD5A2 or only pcDNA3.1, 10μM of 4-OHA (**A**), 4-OHT (**B**), AD (**C**) and T (**D**) were incubated to the medium. This was done in the absence (N-In) or the presence (In) of 10 μM of the inhibitor dutasteride for 3.5 h. The data represents mean values of three different experiments. 4-OHA: 4-hydroxandrostenedione; 4-OHT: 4-hydroxytestosterone; M2: 3β,4β-dihydroxy-5α-androstan-17-one; M3: 3α,4β-dihydroxy-5α-androstan-17-one; Triol: 5α-androstane-3β,4β,17β-triol; AD: 4-androstenedione; T: Testosterone; ADT: androsterone; EPI: Epiandrosterone; DHT: dihydrotestosterone; 3α-diol: 3α-androstanediol; 3β-diol: 3β-androstanediol; 5α-A: 5α-androstanedione.

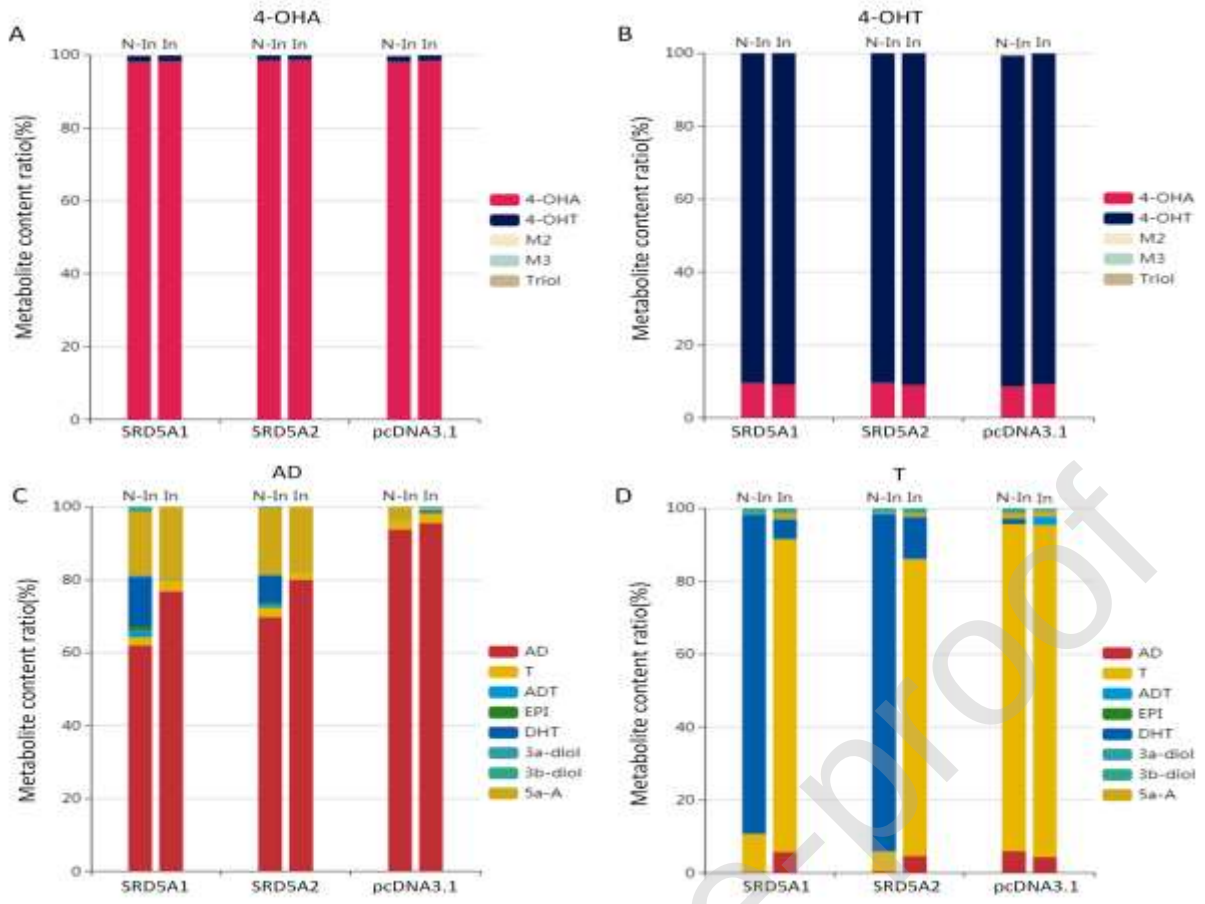

Fig.3 Binding affinities of 4-OHA and 4-OHT to AKR1Cs measured by microscale thermophoresis. The Kd values for the ligands (4-OHA and 4-OHT) and the receptors (AKR1Cs) were calculated using the mass action equation via NanoTemper software from duplicate reads of triplicate experiments. **A-D**: binding affinity between 4-OHA and AKR1C1, AKR1C2, AKR1C3, and AKR1C4,respectively. **E-H**: binding affinity between 4-OHT and AKR1C1, AKR1C2, AKR1C3, and AKR1C4,respectively. 4-OHA: 4-hydroxandrostenedione; 4-OHT: 4-hydroxytestosterone.

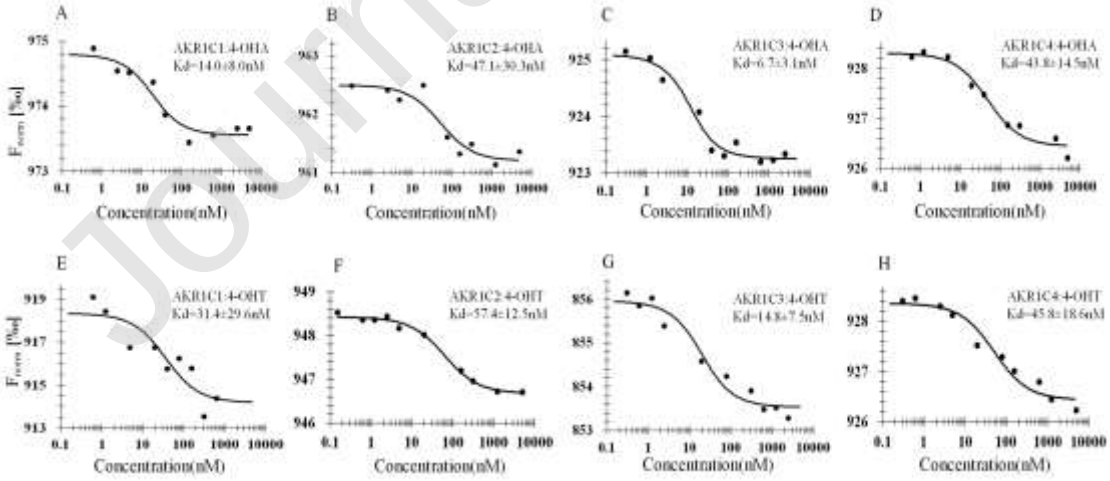

Fig.4 Recovery and identification of metabolites from the culture-medium of COS-1 cells after transfection with the four aldo-keto reductases. After transfection of COS-1 cells for 48h with pcDNA3.1-AKR1Cs or pcDNA3.1, 10μM of 4-OHA (**A**), 4-OHT (**B**), AD (**C**), DHT (**D**) and T (**E**)were

incubated to the medium for 3.5h. This was done in the absence (N-In) or in the presence (In) of 100μM flufenamic acid, the inhibitor of AKR1C1-AKR1C3, and in case of AKR1C4 in the absence or presence of 100μM of the inhibitor phenolphthalein. The data represents the mean values of three different experiments. 4-OHA: 4-hydroxandrostenedione; 4-OHT: 4-hydroxytestosterone; M2: 3β,4β-dihydroxy-5α-androstan-17-one; M3: 3α,4β-dihydroxy-5α-androstan-17-one; Triol: 5α-androstane-3β,4β,17β-triol; AD: 4-androstenedione; T: Testosterone; ADT: androsterone; EPI: Epiandrosterone; DHT: dihydrotestosterone; 3α-diol: 3α-androstanediol; 3β-diol: 3β-androstanediol; 5α-A: 5α-androstanedione.

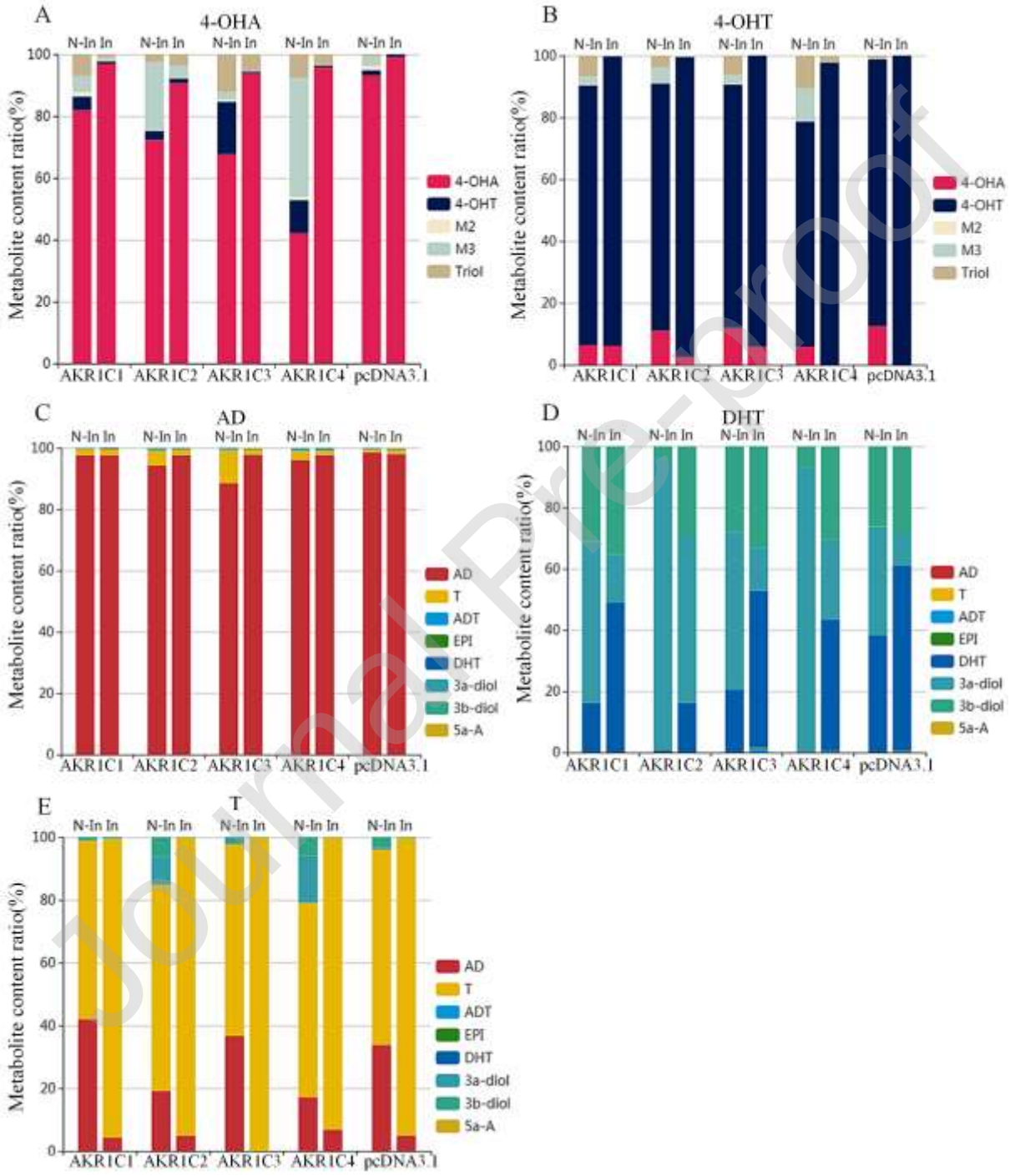

Fig.5 Activities of purified aldo-keto reductases to 4-OHA, 4-OHT, AD and other natural androgens. 50μM of 4-OHA (**A**), 4-OHT (**B**), AD (**C**), DHT (**D**) and T (**E**) were incubated for 3.5 h in the presence

(In) or absence (N-In) of 100 μM flufenamic acid, the inhibitor of AKR1C1-AKR1C3 or of 100 μM of the inhibitor of AKR1C4 phenolphtalein. The reaction system was 200 μL at pH 7.4 containing 200 μM NADPH and 24 μg of purified AKR1C-enzymes. The results represent the mean values of three different experiments. 4-OHA: 4-hydroxandrostenedione; 4-OHT: 4-hydroxytestosterone; M2: 3β,4β-dihydroxy-5α-androstan-17-one; M3: 3α,4β-dihydroxy-5α-androstan-17-one; Triol: 5α-androstane-3β,4β,17β-triol; AD: 4-androstenedione; T: Testosterone; ADT: androsterone; EPI: Epiandrosterone; DHT: dihydrotestosterone; 3α-diol: 3α-androstanediol; 3β-diol: 3β-androstanediol; 5α-A: 5α-androstanedione.

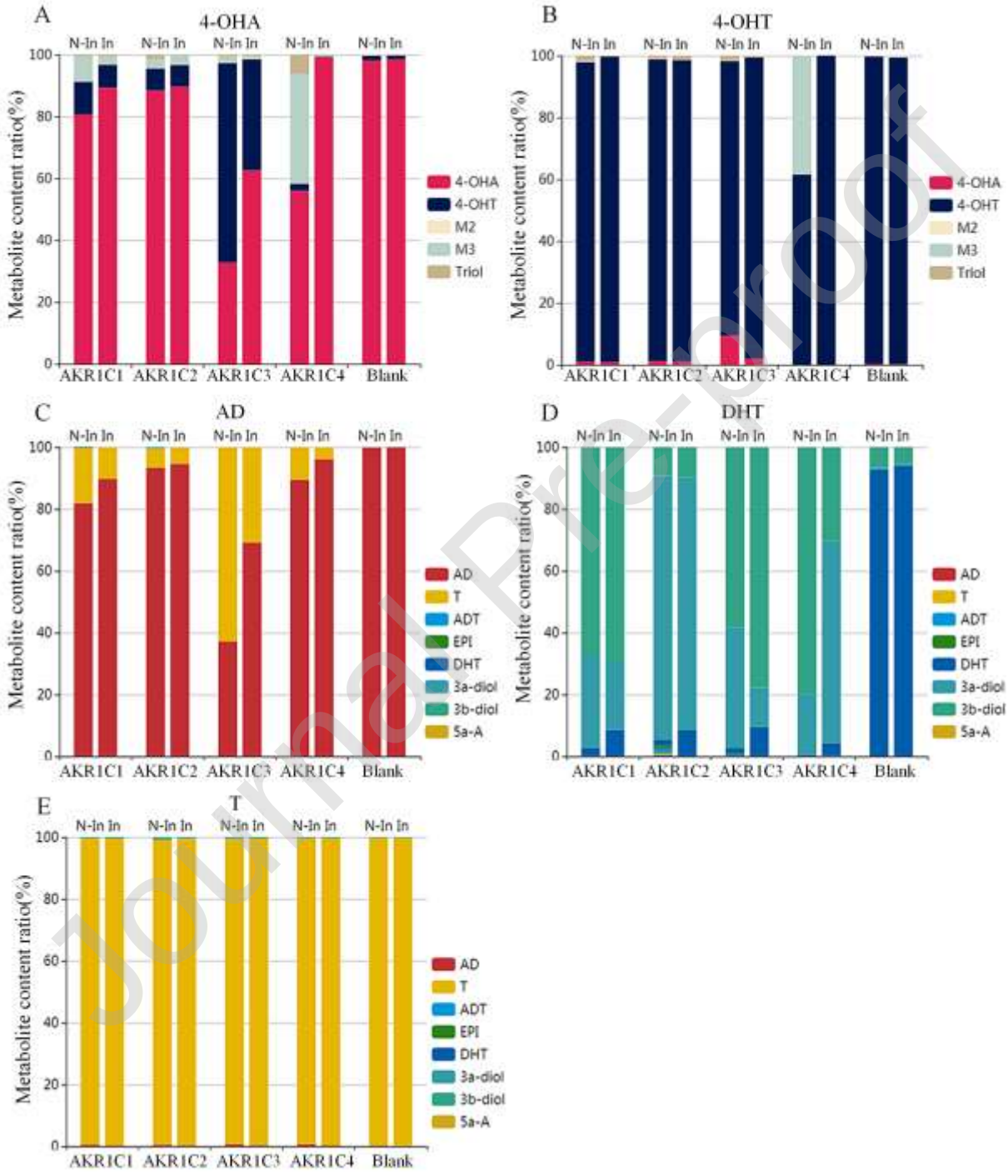

Table 1 Steady-state kinetic parameters for the four alde-keto reductases obtained from reduction of 4-OHA, 4-OHT, AD, DHT and T.

Enzyme	Substrate	K_m(μM)	V_{max}(nmol/min/mg)	Kcat(min^{-1})	Kcat/Km(min^{-1}·mM^{-1})
AKR1C1	4-OHA	8.43	39.75	1.47	174.47
	4-OHT	6.03	12.64	0.47	77.56
	AD	N.D.	N.D.[a]	N.D.	N.D.
	DHT	16.00	37.18	1.38	85.98
	T	N.D.	N.D.	N.D.	N.D.
AKR1C2	4-OHA	33.62	52.27	1.93	57.53
	4-OHT	26.87	41.08	1.52	56.57
	AD	N.D.	N.D.	N.D.	N.D.
	DHT	10.29	28.33	1.05	101.87
	T	N.D.	N.D.	1.93	57.53
AKR1C3	4-OHA	2.30	8.41	0.31	135.29
	4-OHT	N.D.	N.D.	N.D.	N.D.
	AD	2.12	6.34	0.23	110.65
	DHT	11.65	14.24	0.53	45.23
	T	N.D.	N.D.	N.D.	N.D.
AKR1C4	4-OHA	9.77	27.7	1.02	104.90
	4-OHT	6.22	16.41	0.61	97.62
	AD	N.D.	N.D.	N.D.	N.D.
	DHT	8.84	42.74	1.58	178.89
	T	N.D.	N.D.	N.D.	N.D.

a: N.D., Not Detectable. 4-OHA: 4-hydroxandrostenedione; 4-OHT: 4-hydroxytestosterone; AD: 4-androstenedione; DHT: dihydrotestosterone; T: Testosterone.